

# Feasibility of Measuring Particulate Matter Concentrations in Home Kitchens

Jack Williams, Weichen Gao, Chang Liu

## Abstract

Particulate matter (PM) can cause health issues if people are exposed in an environment with a high concentration for a long period of time, and therefore it is important to monitor and record PM concentrations. In this study we established the feasibility of monitoring PM concentrations with easy-to-acquire hardware and self-assembled circuits during and after cooking in a home kitchen. We assembled a data collection device that includes a PMS5003 particulate matter sensor, a real time clock, and a BME680 sensor. The device is controlled by a software we wrote using the Arduino programming environment. It is observed that PM concentrations grow during the cooking and decay exponentially thereafter. We have also observed that concentrations of particulate matter of different sizes and VOC concentrations generally follow the same trend. PMs of different sizes also have almost the same distribution throughout the cooking process. Furthermore, we have discovered that temperature, humidity, and pressure are not significantly affected by the cooking events. Further research could be done on considering the effects of ventilation, different cooking ingredients, and the stove temperature on the PM concentrations. Commercial kitchens might also consider building such PM concentration monitors that give warnings if PM concentrations are at a high level for a significant period of time, and relevant regulatory or advisory standards on PM concentrations in commercial kitchens might be important to be developed.

## 1. Background and Introduction

Particulate matter (PM) pollution is a significant public health concern. PM is generally classified by its aerodynamic diameter, according to which it is characterized as coarse PM (PM<sub>10</sub>) with a diameter between 2.5  $\mu\text{m}$  and 10  $\mu\text{m}$ , and fine PM (PM<sub>2.5</sub>) with a diameter smaller than 2.5  $\mu\text{m}$ . The diameter is directly related to its ability to travel in the atmospheric environment and its ability to be inhaled by humans. The chemical compositions of PM are extremely diverse, with PM<sub>2.5</sub> mainly composed of sulfate, nitrate, ammonium, hydrogen ion, elemental carbon, organic compounds, metal, and particle-bound water, and PM<sub>10</sub> is mainly composed of dust, coal and oil ash, metal oxides, table salt and sea salt, pollen, mold spores, and plant parts (Kim, Kabir, and Kabir 137). The sources of PM pollution are also diverse, including combustion of fossil fuel, organic processes, industrial processes, farming, mining, construction, etc. (Kim, Kabir, and Kabir 137).

It is known that PM pollution adversely affects human health. PM particles are able to penetrate and deposit on the respiratory tract and it is generally believed that smaller particles can penetrate deeper. For particulate matter larger than 10  $\mu\text{m}$  in diameter, the cilia and the mucus in the respiratory tract act to stop the particles, generally collecting the particles in the nose and

throat, where they can be eliminated later through sneezing and coughing. Therefore, it is generally agreed that particulate matter smaller than 10  $\mu\text{m}$  in diameter are those having the most adverse health effects (Kim, Kabir, and Kabir 138). Such particles, depending on their size, could settle in the tracheobronchial tree, in the lung, or even in the bloodstream. In such positions, they may interfere with gas exchange in the lung or even penetrate the lung. Metals in the PM, especially iron, may also cause cellular and tissue damage, leading to inflammation. Certain organic materials in the PM may also cause airway inflammation and malfunction. These may lead to severe health effects, for example pulmonary fibrosis and other lung diseases. Moreover, adverse effects of PM on lung development in children have been observed as well. They may also lead to cardiovascular diseases (Kim, Kabir, and Kabir 138). Indeed, correlation between higher PM concentration level and increased hospital admissions for numerous diseases has been observed around the world. Higher concentration of PM<sub>2.5</sub> is also linked to lower life expectancy (Kim, Kabir, and Kabir 138-139).

Responding to such adverse health effects, Environmental Protection Agency, pursuant to the Clean Air Act, publishes and maintains National Ambient Air Quality Standards. The primary standards, which provide public health protection, were set at 12.0  $\mu\text{g}/\text{m}^3$  in average per year and 35  $\mu\text{g}/\text{m}^3$  in average per 24 hours for PM<sub>2.5</sub>, and 150  $\mu\text{g}/\text{m}^3$  in average per 24 hours for PM<sub>10</sub> (EPA, “NAAQS Table”). EPA also publishes and forecasts PM concentration levels across the US (AirNow).

While outdoor PM concentration is a significant public health issue, indoor PM concentration can be significantly higher than outdoor during several household activities, and in particular cooking. If a fuel-consuming stove is used, depending on the specific fuel that is used, the PM concentration might increase up to 2,000  $\mu\text{g}/\text{m}^3$  (Kim, Kabir, and Kabir 137). It is not clear, though, whether such a high increase will also be present in case an electrical stove is used. Indeed, most studies seem focused on the use of fuel in the cooking process. However, it is known that the burning of food and oil can in itself generate fine particulate matter (Kim, Kang, and Kim 843). Therefore, it is important to collect further data on the particulate matter generated by the cooking process when an electrical stove is utilized.

The aim of this current study is to establish the feasibility of using commercially available sensors and self-assembled circuits to collect data on indoor air quality when cooking is underway and after cooking. Since sizes of particulate matter are relevant to health effects consideration, we collected data on different sizes of particles and studied how the concentration of each of them changes over time and relative to each other. We also studied the decay in the concentration of these particles after the cooking was finished. The data were then evaluated and compared against relevant standards to see whether usual cooking activities might cause a PM exposure exceeding those standards. Our conclusion is that the data collection is feasible and the PM concentrations would indeed be higher during the cooking process. We also confirmed the PM concentration would grow at the beginning of the cooking procedure and also decay

exponentially at the end of the process. In most cases, our results show that the distribution of PM particle sizes stays the same unless certain new PM sources are introduced. Further research into this topic might be conducted by observing the health of people who frequently cook in the long term, doing experiments in more controlled environments, and taking the temperature of stoves and ingredients into account. Our study also proves it possible to set up a PM concentration monitoring device in commercial kitchens to alert the kitchen staff when the PM concentrations exceed safety standards.

## 2. Methods and Procedures

### 2.1. Hardware

The hardware we need for this research is a device that can conveniently collect all the relevant data so that we can analyze and compare between different data runs and data categories. Our aim is to present a technical analysis of airborne particulate concentrations in home kitchens, so our device should be able to collect data on airborne particulate matters that includes PM2.5, PM10 and so on. The particulate matter sensor PMS5003 satisfies these requirements. We would need to store the data in a useful format and here we used an SD card onto which we could write data that we could then process. To control device components and receive data from them, we need a microcontroller and we used the Arduino Mega 2560 controller to do this task. To communicate with our device effectively, we used a keypad to give commands and an LCD screen to display the data from our device.

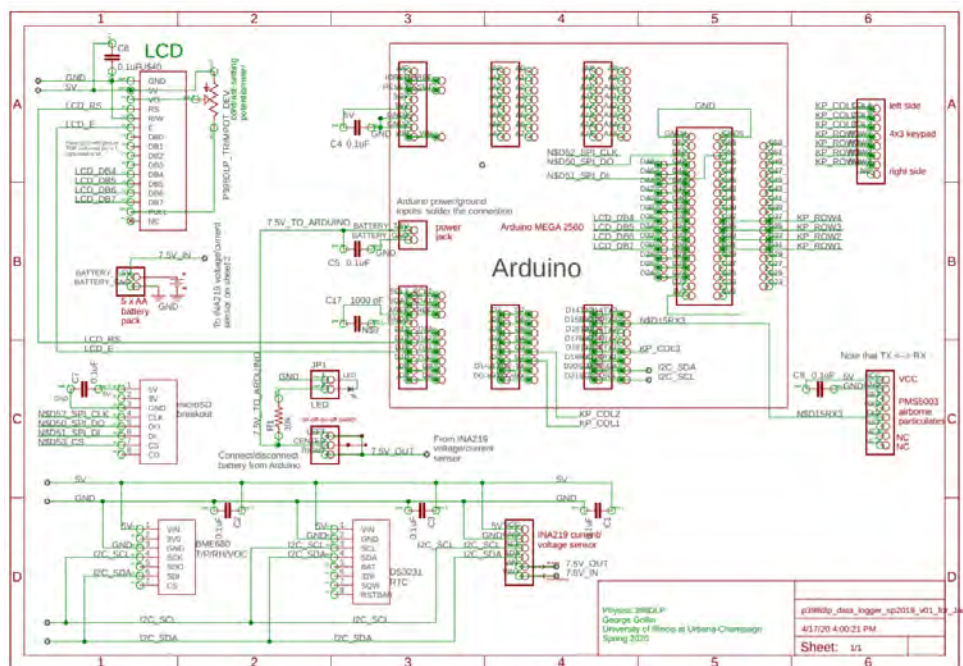


**Fig 2.1.** The schematic diagram for the data collection device.



**Fig 2.2.** Front view of the data collection device.



**Fig 2.3.** Back view of the data collection device.

### 2.1.1. PMS5003

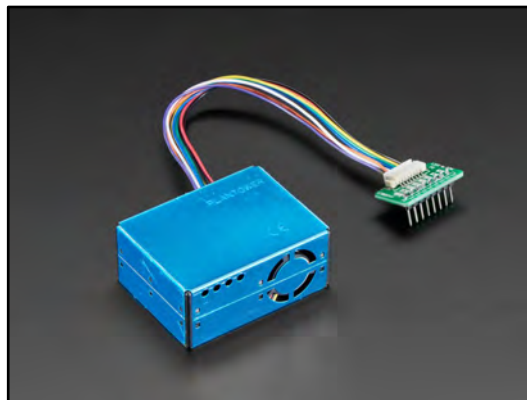


**Fig. 2.4.** PMS5003 (Adafruit Industries, “PM2.5 Air Quality Sensor and Breadboard Adapter Kit - PMS5003”).

The PMS5003 provides us with data of PM1.0, PM2.5 and PM10 concentrations in both standard and environmental units, and it also gives us the number of particulate matters (PMs) per 0.1 liter of air. The second type of data would be categorized in 0.3  $\mu\text{m}$ , 0.5  $\mu\text{m}$ , 1.0  $\mu\text{m}$ , 2.5  $\mu\text{m}$ , 5.0  $\mu\text{m}$  and 10.0  $\mu\text{m}$  size bins. This device is key to our research because it can collect the PM concentration data we require in many forms and also distinguish between different sizes of PM. With this sensor, we could establish relations between the amounts of particulate matters of different sizes and what ingredients were cooked or which cooking methods were used. Since the sensor could update the PM count every second, it is possible to analyze how fast particulate matters spread throughout the kitchen, how quickly the concentration increases to the peak level and how long it takes for the concentration to decay back to the baseline level. The sensor uses laser scattering to radiate floating particles near it in the air, and then collect scattered light to obtain PM concentrations. The microcontroller inside the sensor calculates the diameters of particles and the number of particles of different sizes per volume (Adafruit Industries, “PM2.5 Air Quality Sensor and Breadboard Adapter Kit - PMS5003”).

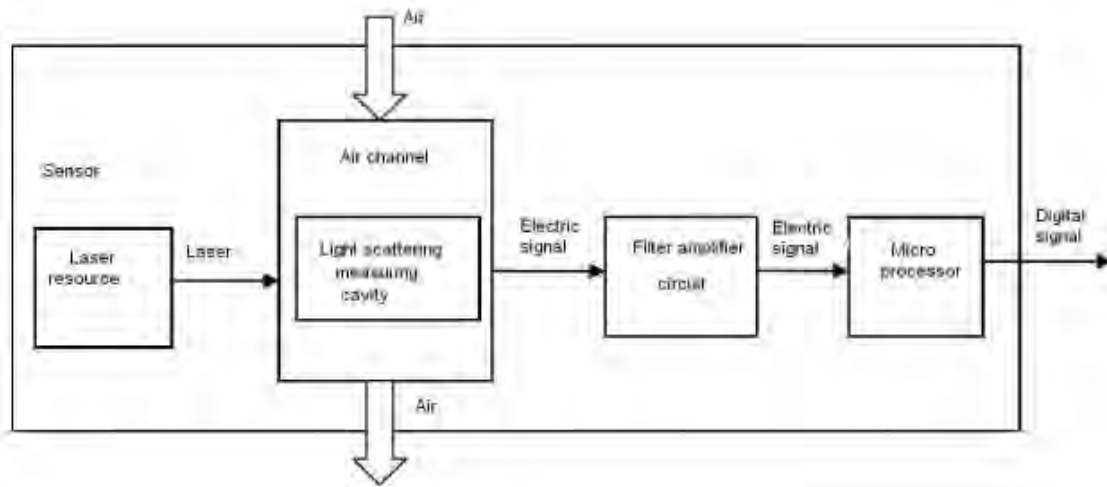


**Fig. 2.5.** Block diagram of PMS5003 (Plantower Technology 2).

### 2.1.2. BME680

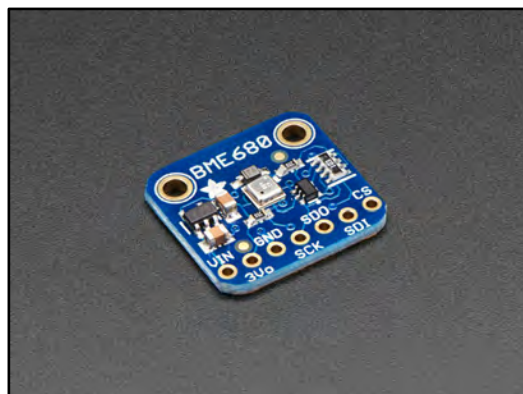


**Fig. 2.6.** BME680 (Adafruit Industries, “Adafruit BME680 - Temperature, Humidity, Pressure and Gas Sensor”).

This is a low power gas, pressure, temperature, and humidity sensor. BME 680 is needed to study the relations between the concentrations of particulate matters and the VOC gas concentration, pressure, temperature, and humidity of the kitchen. The temperature measurement is important also for the reason that the temperature information is often used to compensate for the temperature influences in other parameters. The sensor can measure humidity with  $\pm 3\%$  accuracy, barometric pressure with  $\pm 1$  hPa absolute accuracy, and temperature with  $\pm 1.0^\circ\text{C}$  accuracy. Its response rate is less than 1s for new sensors, and this could help us analyze data on a smaller time scale with greater precision. The BME680 is also small in dimension and requires low power which is helpful since we want to integrate the sensor into a hand-held device that is powered by batteries. This sensor, like all VOC gas sensors, has variability and has to be calibrated against known sources if accurate data is needed (Adafruit Industries, “Adafruit BME680 - Temperature, Humidity, Pressure and Gas Sensor”).

### 2.1.3. Arduino Mega 2560

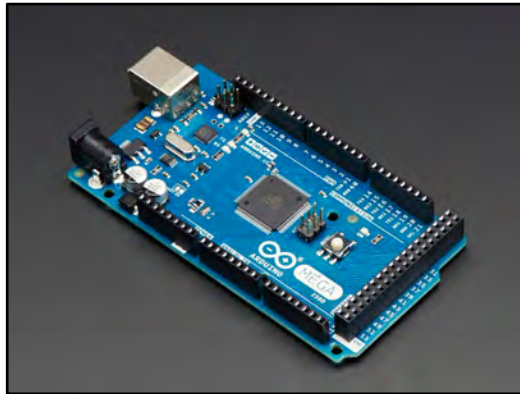


**Fig. 2.7.** Arduino Mega 2560 (Arduino).

The Arduino microcontroller controls all the hardware we installed on the printed circuit board. Its function is to execute the series of commands we have written in C programming language using the Arduino IDE. It has 54 digital input/output pins and 16 analog pins. It has a USB connection which is used to upload the software instructions to the microcontroller (Arduino).

### 2.1.4. DS3231 Real Time Clock

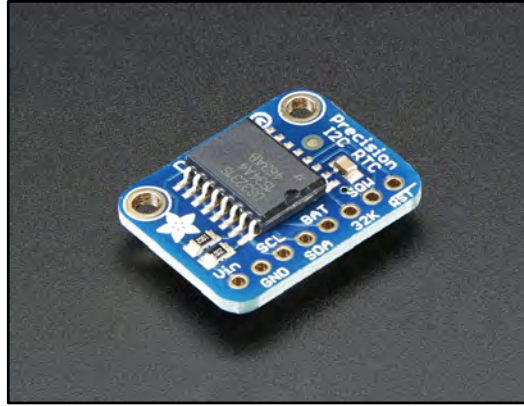


**Fig. 2.8.** DS3231 real time clock (Adafruit Industries, “Adafruit DS3231 Precision RTC Breakout”).

The DS3231 real time clock provides our data collection software with accurate and precise timing. It is needed to track what happened during the cooking process and analyze the connections between those events and the PM concentrations. It would reset the time if the power is cut off, so a coin cell is needed (Adafruit Industries, “Adafruit DS3231 Precision RTC Breakout”).

#### 2.1.5. INA219 Current Sensor

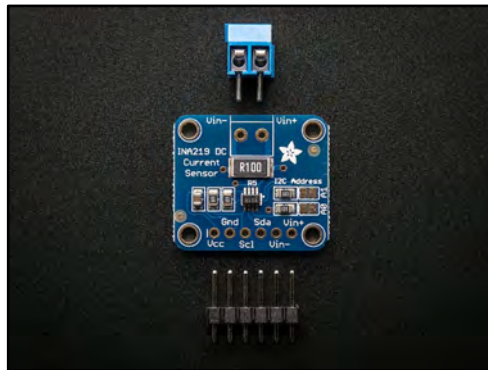


**Fig. 2.9.** INA219 current sensor (Adafruit Industries, “INA219 High Side DC Current Sensor Breakout - 26V  $\pm$ 3.2A Max”).

The INA219 high side DC current sensor breakout enables us to measure the power use of our device. It will measure the battery voltage, the current draw, and the power draw. It measures high side voltages and DC currents with a precision of 1% and also tracks battery life (Adafruit Industries, “INA219 High Side DC Current Sensor Breakout - 26V  $\pm$ 3.2A Max”).

#### 2.1.6. LCD Screen

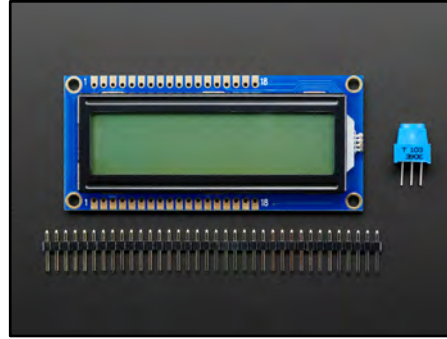


**Fig. 2.10.** The LCD screen (Adafruit Industries, “RGB Backlight Positive LCD 16 x 2 + Extras - Black on RGB”).

The LCD functions as a screen that displays information about the working status of the data collection device. It can report data during the data collection, and give notices when the device starts or stops collecting data. The screen’s size is 27mm x 71mm / 1.1" x 2.8" and it is 16 characters wide with 2 rows (Adafruit Industries, “RGB Backlight Positive LCD 16 x 2 + Extras - Black on RGB”).

### 2.1.7. MicroSD Card



**Fig. 2.11.** The microSD card (Adafruit Industries, “MicroSD Card Breakout Board”).

The SD card helps store the data we have collected. After each data collection run, a CSV file will be generated which could then be used as a data source for analysis.

### 2.1.8. Keypad





**Fig. 2.12.** The keypad (Adafruit Industries, “3 x 4 Phone-style Matrix Keypad”).

The keypad is needed to interact with the data collector without it being connected to the computer. By pressing each of the keys of the keypad, different commands can be given. Such commands include displaying the current time, or starting the data collection. This keypad has 12 buttons, i.e., 3 columns and 4 rows (Adafruit Industries, “3 x 4 Phone-style Matrix Keypad”).

### 2.1.9. PCB

The printed circuit board connects electronic components with copper laminated onto and/or between non-conductive substrates. This device integrates various components within a compact space such that we can make our data collection device hand-held and easy to operate (“PCB Layout”). The electronic components are generally soldered to the PCB, but we use female and male headers so that the components can be reused later.

## 2.2. Software

### 2.2.1. DAQ Software

The data acquisition (DAQ) software for the data collection devices was programmed in the Arduino programming environment, using C language. The code incorporated previous works by George Gollin.

The program initializes and powers the BME680 sensor, the PMS5003 airborne particulate sensor, the DS3231 real time clock, the INA219 current and voltage sensor, the LCD screen, the SD card reader, and the keypad. It is run from an Arduino board installed on the printed circuit board. The program collects data approximately once every second. Depending on the instructions entered through the keypad, it also stores the data in the SD card. It also displays a selected segment of current data on the LCD screen, according to the value of a variable `current_mode`, which can be changed through keypad instructions.

### Table 2.1

The 12 keys and the corresponding instructions on the keypad.

Key	Instruction
1	Display on the LCD screen the temperature and pressure readings
2	Display on the LCD screen the relative humidity and VOC gas readings
3	Display on the LCD screen the altitude (as calculated from the pressure) and the number of lines of content that have been written on the LCD screen
4	Display on the LCD screen the PM > 0.3 $\mu\text{m}$ and PM > 0.5 $\mu\text{m}$ readings
5	Display on the LCD screen the PM > 1.0 $\mu\text{m}$ and PM > 2.5 $\mu\text{m}$ readings
6	Display on the LCD screen the PM > 5.0 $\mu\text{m}$ and PM > 10.0 $\mu\text{m}$ readings
7	Display on the LCD screen the PM1.0 and PM2.5 readings
8	Display on the LCD screen the PM10 and device battery voltage readings
9	Display on the LCD screen the device battery current and device battery power (as calculated from the battery voltage and current) readings
*	Display on the LCD screen the air quality indexes (as calculated from the PM2.5 and PM10 readings)
0	Display on the LCD screen the current date and time (as recorded by the RTC)
#	Begin storing the collected data to the SD card, or, if the data storage is already underway, stop the data storage

Each time a key is pressed, one would see some corresponding indication on the LCD screen. For example, when the '#' key is pressed, the LCD screen will display "Saving data" and the name of the file it is currently writing into. If the data storage is already underway, the LCD screen will display "Stop saving data".

If the DAQ software is instructed to save data to the SD card (the variable `saving_data` is set to true by the instruction sent from the keypad), it will collect and save them in a CSV file format. Each line in the file will contain an entry (the first line includes the data labels), and each entry will contain data in the following order: Date, Time, Battery Voltage (V), Battery Current (mA), Battery Power (W), Temperature ( $^{\circ}\text{C}$ ), Pressure (hPa), Relative Humidity (%), VOC Gas (ppb), Altitude (m), PM > 0.3  $\mu\text{m}$  (Particles / 0.1L), PM > 0.5  $\mu\text{m}$  (Particles / 0.1L), PM > 1.0  $\mu\text{m}$

(Particles / 0.1L), PM > 2.5  $\mu\text{m}$  (Particles / 0.1L), PM > 5.0  $\mu\text{m}$  (Particles / 0.1L), PM > 10.0  $\mu\text{m}$  (Particles / 0.1L), PM1.0 ( $\mu\text{g}/\text{m}^3$ ), PM2.5 ( $\mu\text{g}/\text{m}^3$ ), PM10 ( $\mu\text{g}/\text{m}^3$ ), AQI (as calculated from PM2.5 data), AQI (as calculated from PM10 data).

Each time the data storage process begins, the program will create a new file to save the data, with file name `data####.csv`, ranging from `data0000.csv` to `data9999.csv`. Therefore, without replacing the SD card, it is possible to save up to 10,000 data files, so long as the storage capacity of the SD card allows.

All data displayed and stored come directly from the sensors except the battery power and the AQI readings. The battery power is simply obtained by multiplying the battery voltage and the battery current (divided by 1,000 to change the unit from mA to A). The two AQI readings are calculated from the PM2.5 data and the PM10 data, respectively, following the AQI calculation mechanism defined by EPA (EPA, “Technical Assistance Document for the Reporting of Daily Air Quality – the Air Quality Index (AQI)”).

### 2.2.2. Offline Analysis

Offline analysis was completed using Python 3.7 (open source and cross-platform programming language) and the tool Jupyter Notebooks to create an InteractivePython environment for performing our data analysis. We use the scientific modules pandas, numpy, and matplotlib.

Pandas allows us to load and organize our data in the environment using the DataFrame object. The DataFrame object represents a relational table; upon being loaded with data collected from our device, each entry will have all points of data for a certain time. The features used for analyzing airborne particulate concentration were: PM > 0.3  $\mu\text{m}$  (Particles/0.1L), PM > 0.5  $\mu\text{m}$  (Particles/0.1L), PM > 1.0  $\mu\text{m}$  (Particles/0.1L), PM > 2.5  $\mu\text{m}$  (Particles/0.1L), PM > 5.0  $\mu\text{m}$  (Particles/0.1L), PM > 10.0  $\mu\text{m}$  (Particles/0.1L), PM1.0 ( $\mu\text{g}/\text{m}^3$ ), PM2.5 ( $\mu\text{g}/\text{m}^3$ ), PM10 ( $\mu\text{g}/\text{m}^3$ ), AQI (as calculated from PM2.5 data), AQI (as calculated from PM10 data). We also monitored other air quality features: Temperature ( $^{\circ}\text{C}$ ), Pressure (hPa), Relative Humidity, and Volatile Organic Compound Resistivity ( $\text{k}\Omega$ ). Our device also collects data on its own battery voltage, current, and power. However, we saw these as values used for monitoring our device while using it, so they were not included in analysis.

To perform analysis on decay rates, we used the numpy module. Numpy allows us to create additional data points of our airborne particulate data on a logarithmic scale. We then visually cut the growth and decay of each feature so numpy can calculate the best fit curve and resultant growth and decay rates. The values numpy calculates are then used to plot best fit curves.

Graphing was done using matplotlib, a python plotting package for creating animations and visualizations. Most plots were just made as a reading over time, but other data graphing methods were used as well. See **Section 3**.

### 2.3. Data Collection

All data collection runs were conducted in home kitchens. In each run, data on airborne particulate, temperature, pressure, relative humidity, and VOC gas were collected and analyzed.

In each run, the device was turned on for at least a minute before actual data collection began. This was done based on prior observations in test runs that the device needed approximately a minute to fully “fire up”, and the readings on relative humidity and the VOC gas, among other data categories, might be inaccurate barring that.

The device began collecting data about 10 minutes before the actual cooking began, so that an appropriate amount of baseline data can be included. Furthermore, the device was not turned off until at least five minutes after the cooking concluded, so that data on the decay in the airborne particulate content can be collected and analyzed. We have also recorded the whole process of the cooking with our phones. The video also records the time displayed on the data collection device to align the timestamps in our data and the video. This is used to understand when the events recorded in the video happened and how that affected the PM concentration level.

Chang’s cooking process involved heating pot, heating oil, frying pork, frying vegetables, stirring the ingredients, adding salt and sauce, and removing ingredients. These events were recorded and identified in the video to establish connections with the changes in PM concentrations.



**Fig. 2.13.** A photo of Chang’s kitchen.

Jack was responsible for the bread making run. The process involved mixing the dough, kneading it, letting it rise, and then baking it. The events were recorded and can be referenced as a timestamp. The data for the bread making was taken on Monday April 13th at 11am.

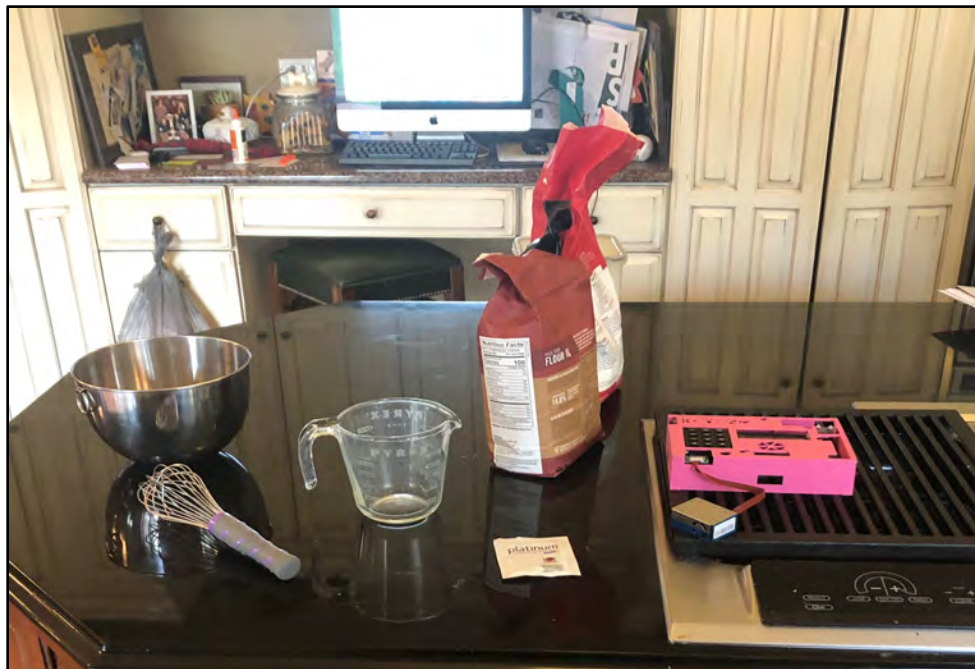


**Fig 2.14.** A photo of Jack's kitchen.

### **3. Results**

#### **3.1. Airborne Particulate Features**

The following graphs plot the airborne particulate data versus time. Also plotted are lines of best fit for the decay of airborne particulates. Decay was modeled in the form of  $y = Ae^{Bt}$ , to give us exponential models of decay.

Right away we were able to see that in runs where meat was being cooked over heat, PM concentrations would spike when ingredients were added to heat. Observations made from the Focaccia Bread run indicate that all-purpose flour is either too large or too small to be detected by the PMS5003. The spike seen near 8000 seconds is the result of the use of non-stick cooking spray. Immediately when it was used, PM concentration spiked very high. It then just as quickly fell.

### 3.1.1. PM1.0 ( $\mu\text{g}/\text{m}^3$ )

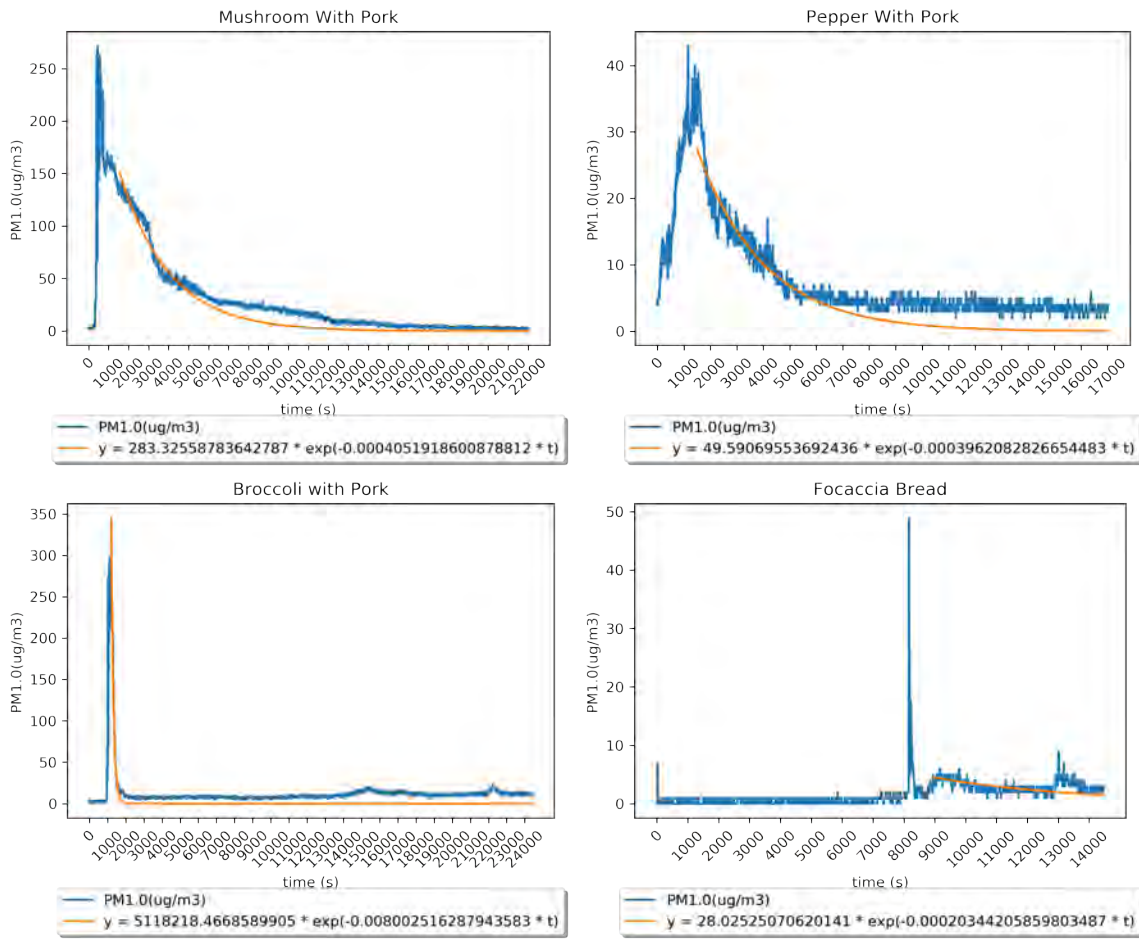


**Fig. 3.1.** PM1.0 ( $\mu\text{g}/\text{m}^3$ ).

**Table 3.1**

Run	Start Time	End Time	Mean	Median	Range
Mushroom	71	788	119.63	157	270
Pepper	34	977	16.55	14	24
Broccoli	141	1185	43.82	3	297
Focaccia	64	13974	1.644	1	49

These graphs show the PM1.0 ( $\mu\text{g}/\text{m}^3$ ) data. This is the concentration of particles of size smaller than 1.0 micrometers, measured in units of micrograms per meter cubed of air.

### 3.1.2. PM2.5( $\mu\text{g}/\text{m}^3$ )

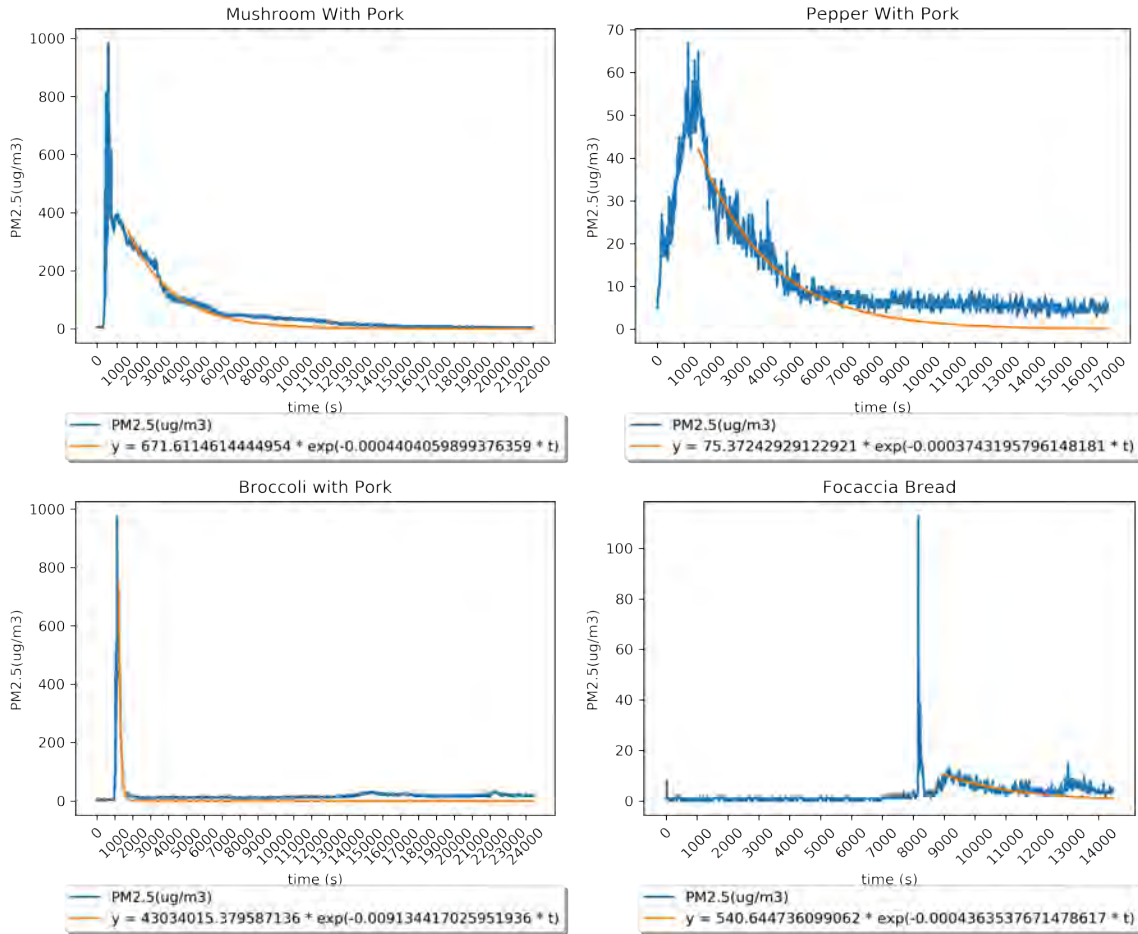


**Fig. 3.2.** PM2.5 ( $\mu\text{g}/\text{m}^3$ ).

**Table 3.2**

Run	Start Time	End Time	Mean	Median	Range
Mushroom	71	788	306.51	354	982
Pepper	34	977	27.1	24	37
Broccoli	141	1185	84.83	5	976
Focaccia	64	13974	3.11	1	113

These graphs show the PM2.5 ( $\mu\text{g}/\text{m}^3$ ) data. This is the concentration of particles of size smaller than 2.5 micrometers, measured in units of micrograms per meter cubed of air.

### 3.1.3. PM10 ( $\mu\text{g}/\text{m}^3$ )

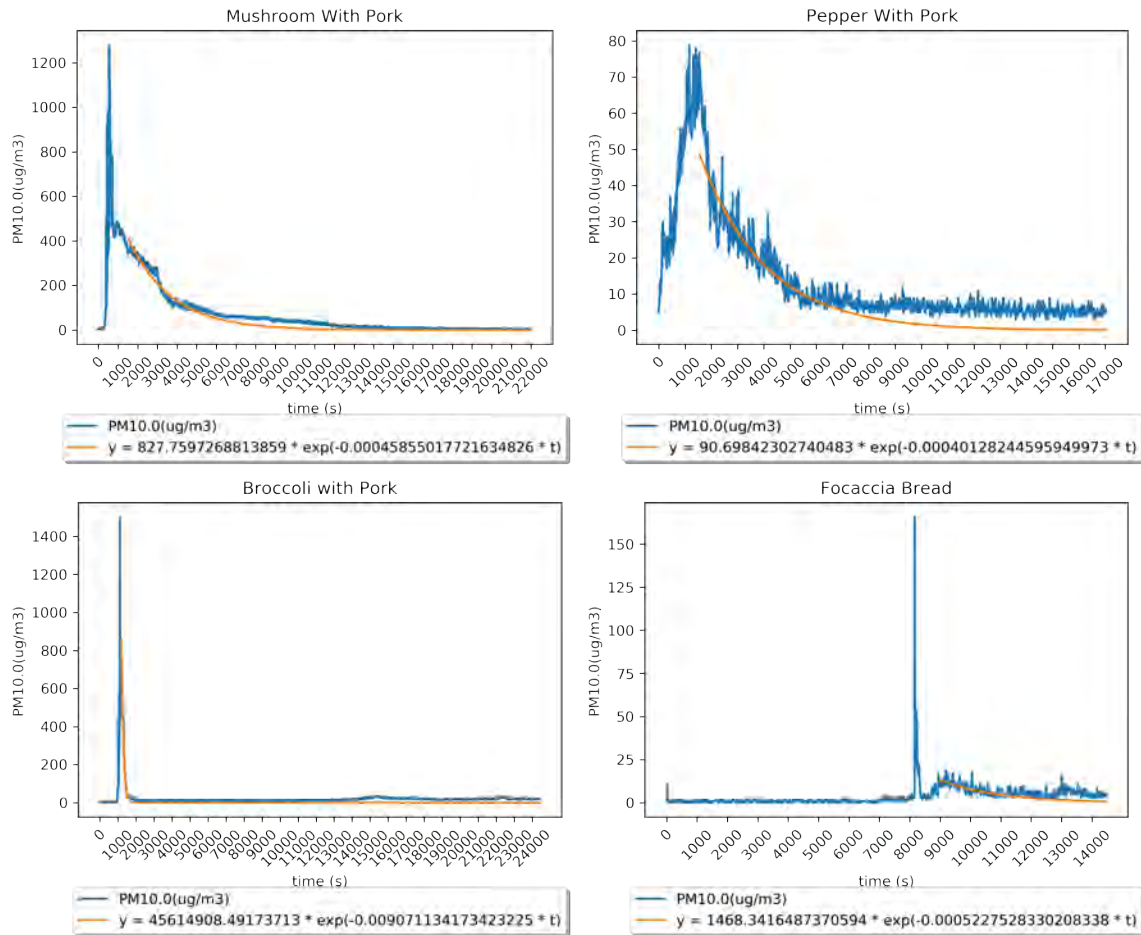


**Fig. 3.3.** PM10 ( $\mu\text{g}/\text{m}^3$ ).

**Table 3.3**

Run	Start Time	End Time	Mean	Median	Range
Mushroom	71	788	371.39	389	1278
Pepper	34	977	31.44	27	46
Broccoli	141	1185	99.04	5	1502



Focaccia	64	13974	3.8	2	166
----------	----	-------	-----	---	-----

These graphs show the PM10 ( $\mu\text{g}/\text{m}^3$ ) data. This is the concentration of particles of size smaller than 10 micrometers, measured in units of micrograms per meter cubed of air.

### 3.1.4. PM Size Counts

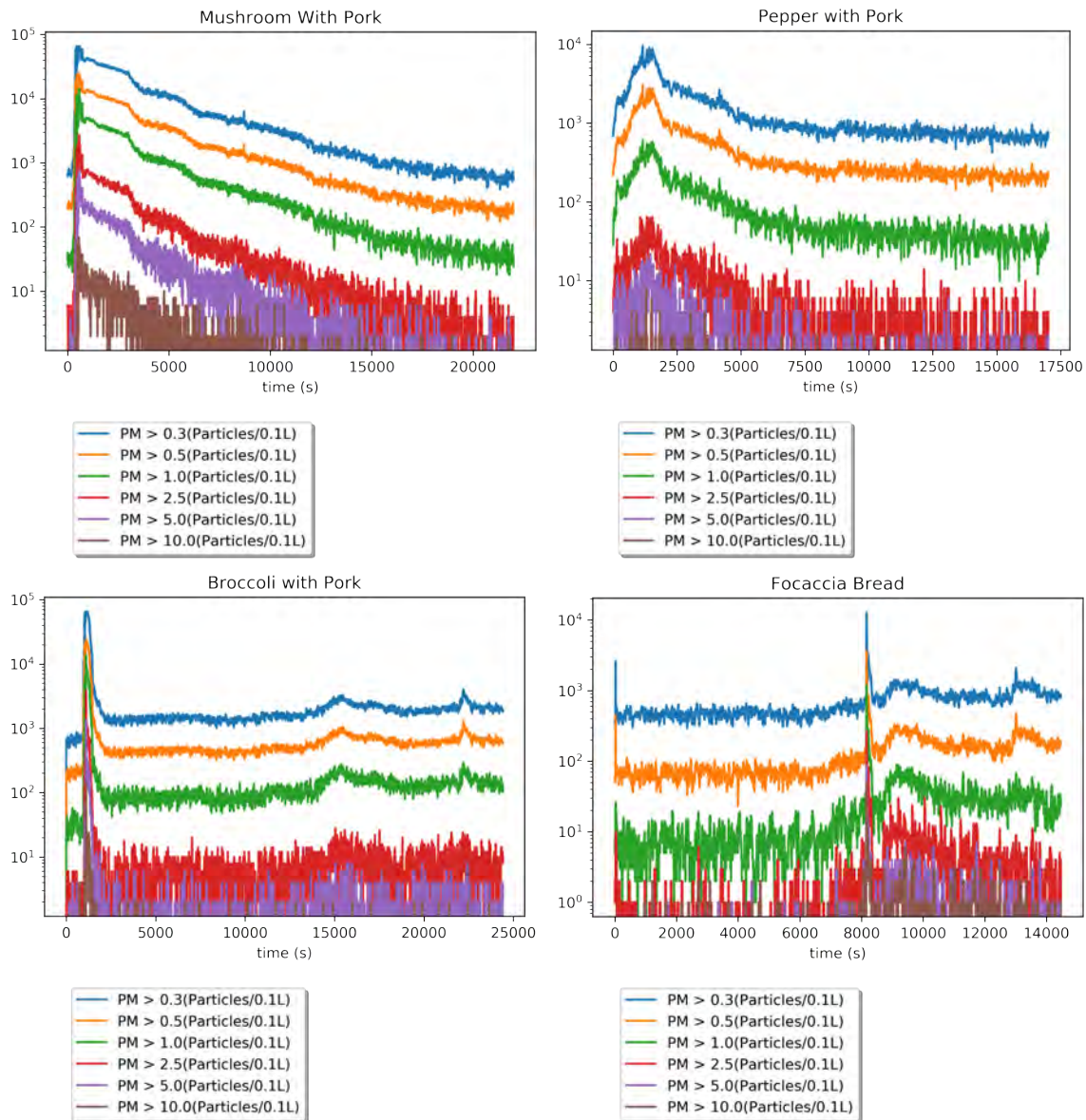


**Fig. 3.4.** Particle size counts graphed on a log scale.

These graphs represent particle counts grouped by size. Each reading represents the count of particles above a certain size (in units of micrometers). The concentration is measured in

particles per 0.1 liters of air. We elected to graph these on a log scale as they have the same shape as the PM1.0, PM2.5, and PM10 graphs, and we wanted to show this shape on a log scale.

### 3.1.5. AQI (PM2.5)

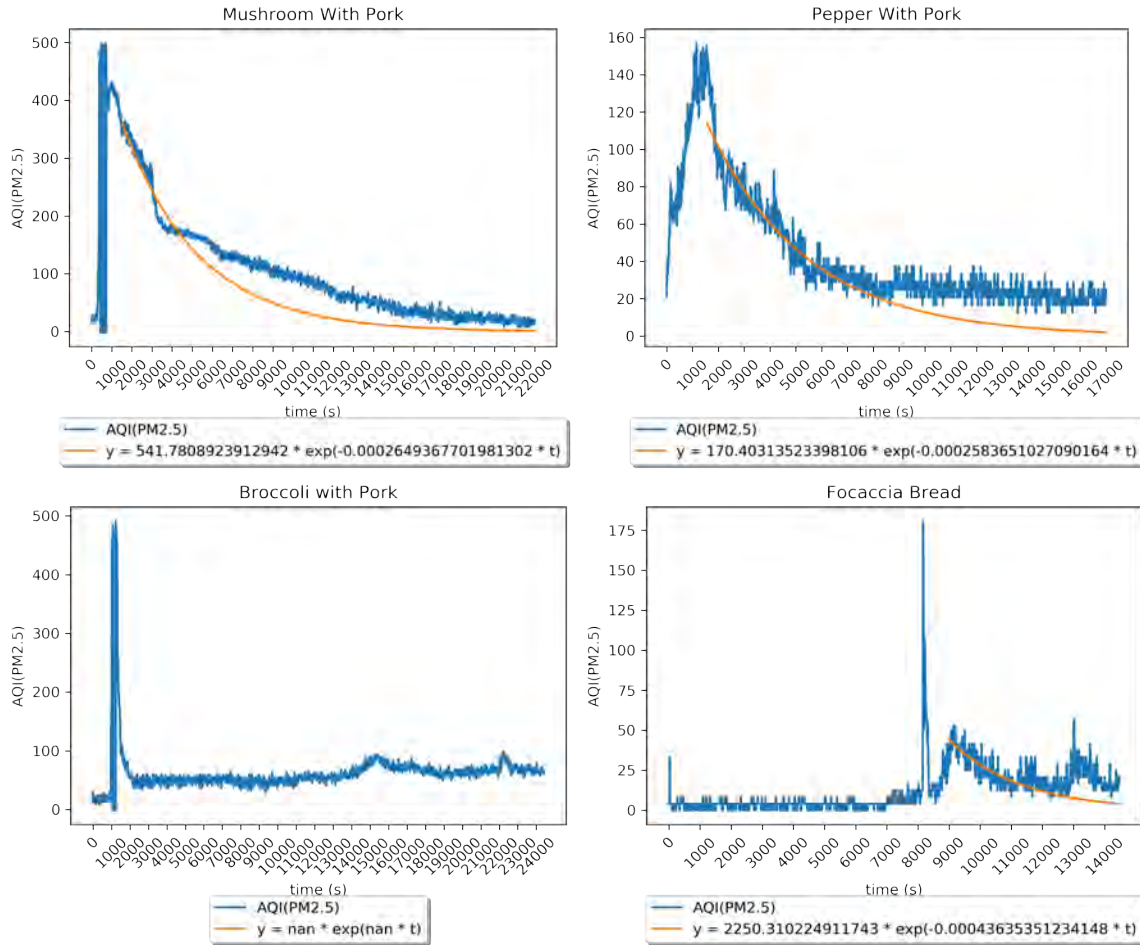


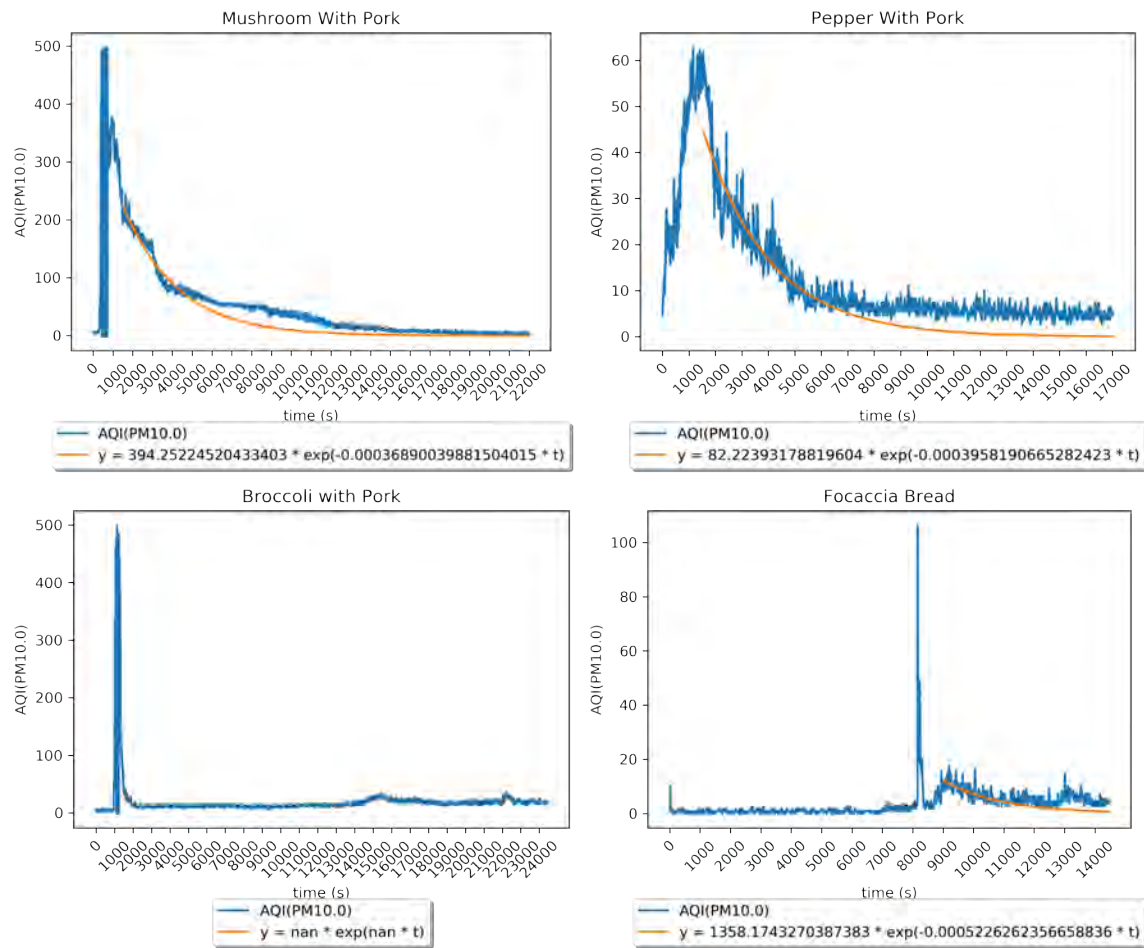
Fig. 3.5. Air Quality Index (calculated from PM2.5).

Table 3.4

Run	Start Time	End Time	Mean	Median	Range
Mushroom	71	788	140.98	25.0	500.08
Pepper	34	977	82.9	76.03	91.06
Broccoli	141	1185	50.5	20.83	485.55
Focaccia	64	13974	12.57	4.17	180.69

Air quality index calculated from PM2.5 concentration. The Air Quality Index has a maximum of 500, so when the value calculated was higher, our software would overwrite this value to 0 to show this. This can be seen in the Mushroom and Broccoli runs (**Fig. 3.5**).

### 3.1.6. AQI (PM10)



**Fig. 3.6.** Air Quality Index (calculated from PM10).

**Table 3.5**

Run	Start Time	End Time	Mean	Median	Range
Mushroom	71	788	103.16	6.48	499.0
Pepper	34	977	29.11	25.0	42.23

Broccoli	141	1185	29.12	4.63	501.0
Focaccia	64	13974	3.48	1.85	106.44

Air quality index calculated from PM10 concentration. The Air Quality Index has a maximum of 500, so when the value calculated was higher, our software would overwrite this value to 0 to show this. This can be seen in the Mushroom and Broccoli runs (**Fig. 3.6**).

### 3.1.7. PM Concentration Decay

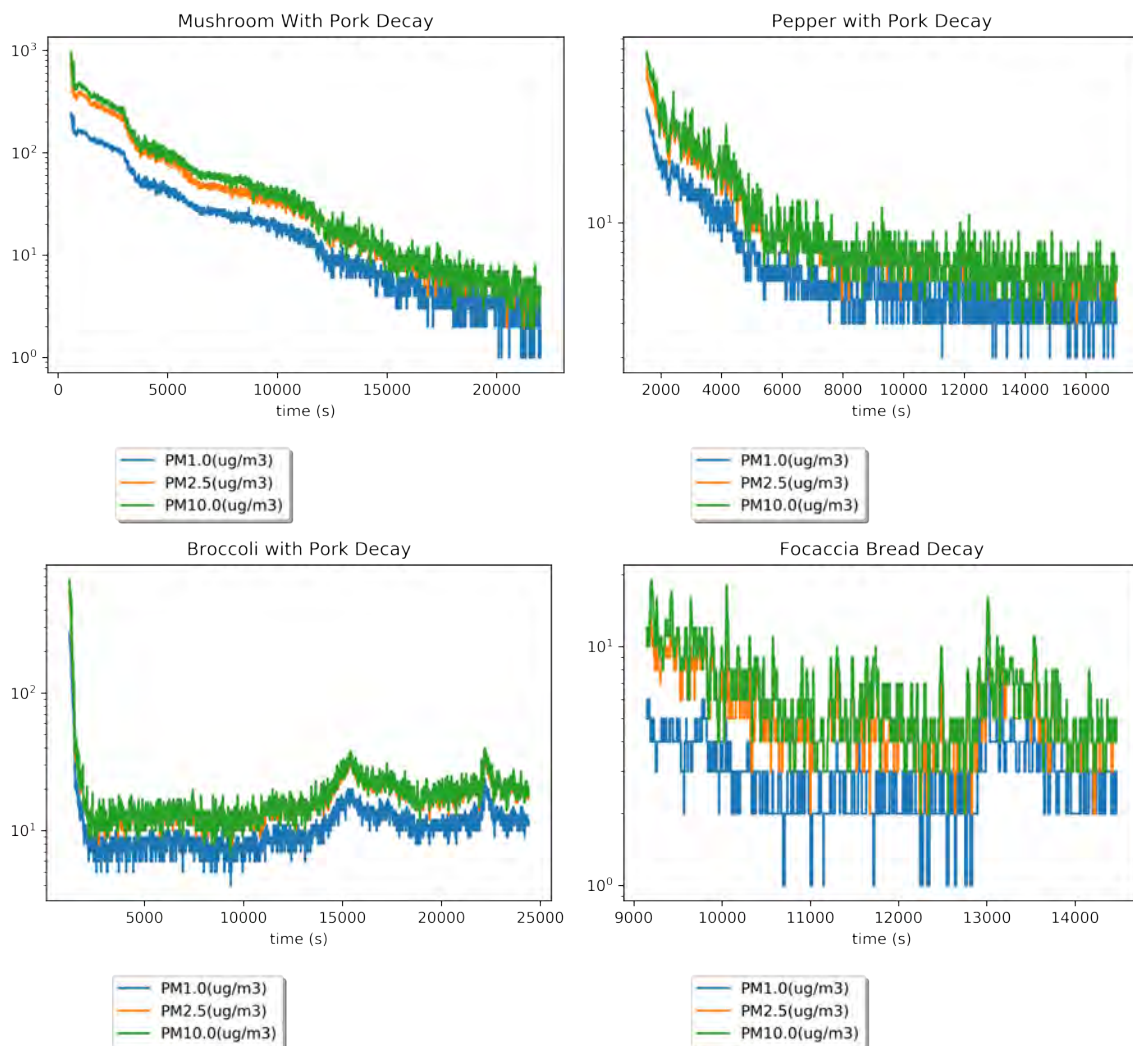


**Fig 3.7.** Decay of PM1.0, PM2.5, and PM10 on a log scale.

These graphs show the decay of each data run graphed on a log scale. In each run, details align between PM1.0, PM2.5, and PM10 concentrations.

### 3.1.8. Distribution of Particle Sizes

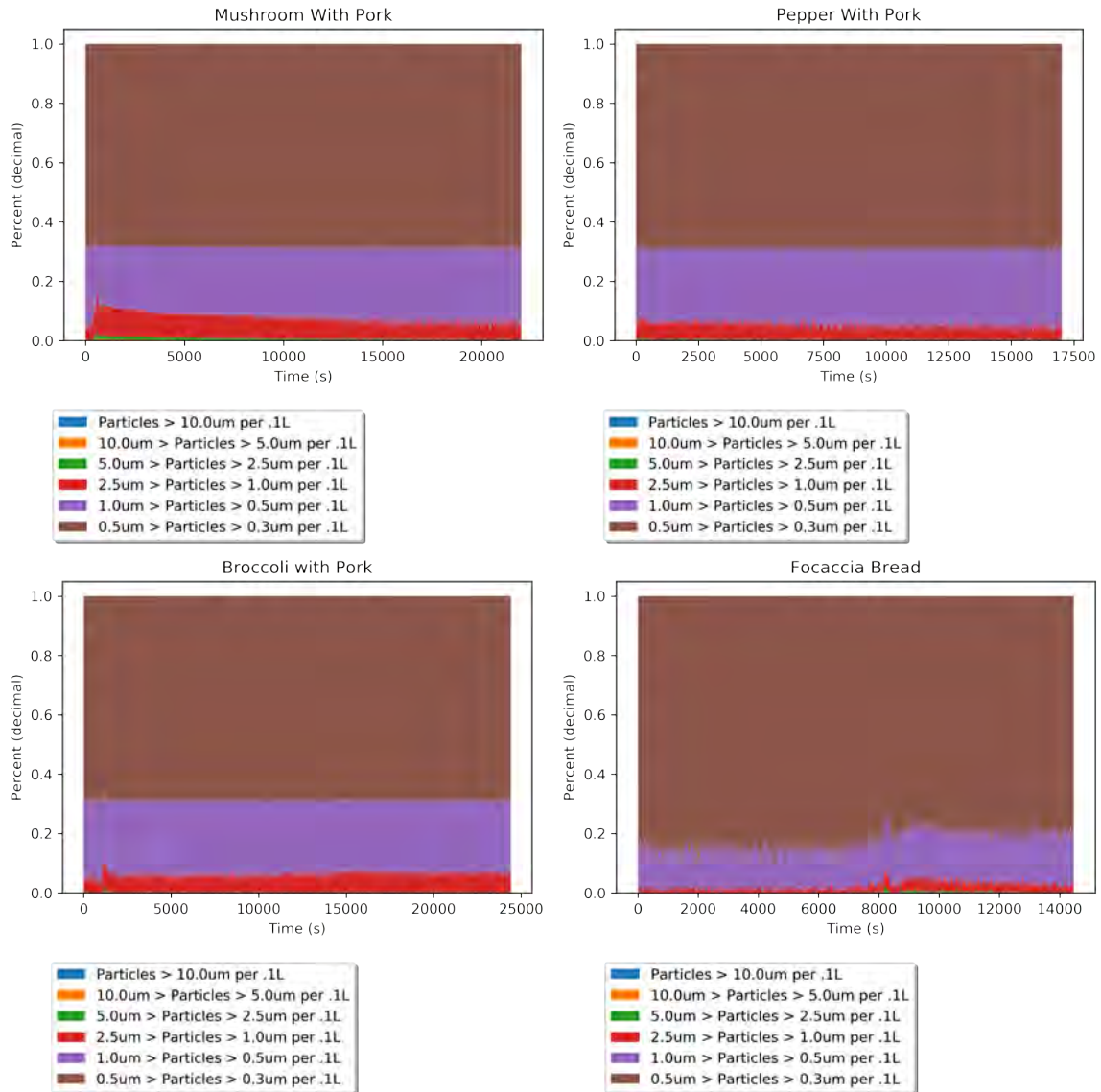


**Fig. 3.8.** Distributions of particles by size over time.

Particle distribution by size. It can be seen that for the most part, the size distribution remains unchanged, regardless of the amount of particles, indicating that particulate matters of all sizes decay at the same rate.

## 3.2. Other Air Features

### 3.2.1. Temperature (°C) and Relative Humidity

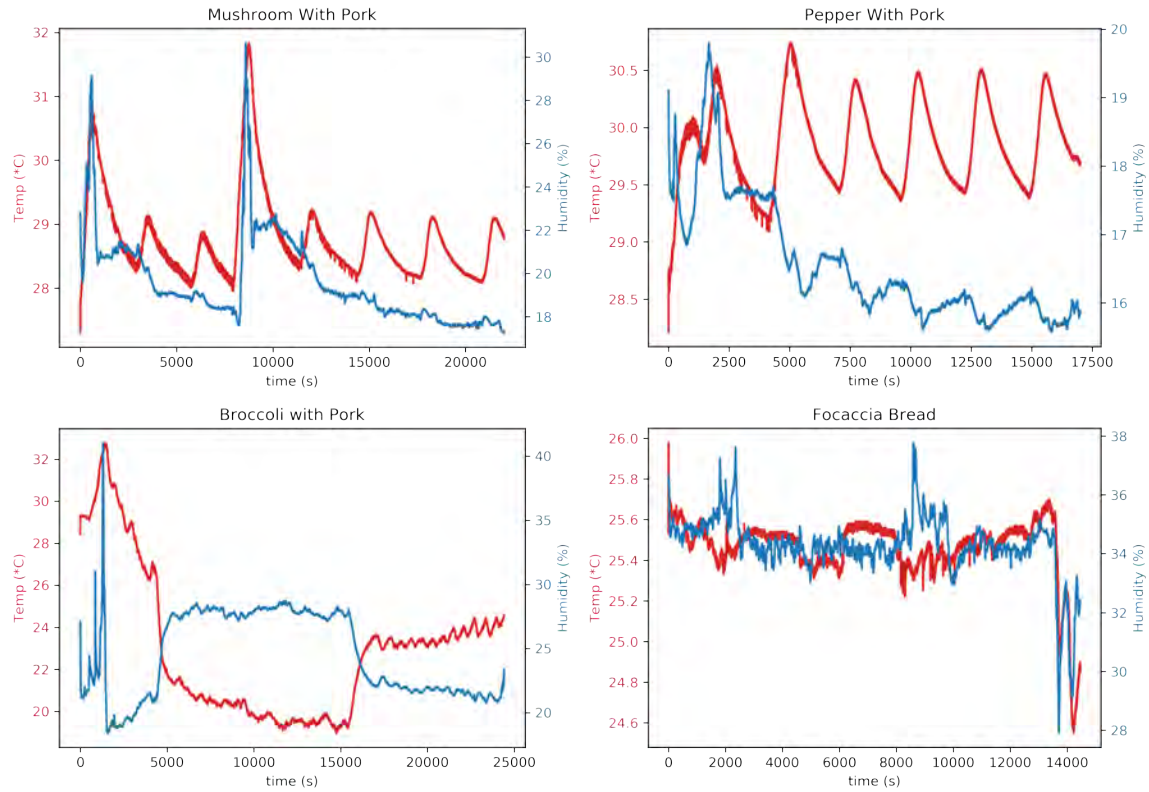


**Fig. 3.9.** Temperature and relative humidity graphed together.

These plots show the relationship between temperature and relative humidity. It can be seen that in the long term, they follow each other. However, for short perturbations they will be inversely correlated. Periodic behavior in temperature in the Mushroom and Pepper runs could probably be attributed to air conditioning. In most cases relative humidity will not change much.

### 3.2.2. Volatile Organic Compound Resistivity

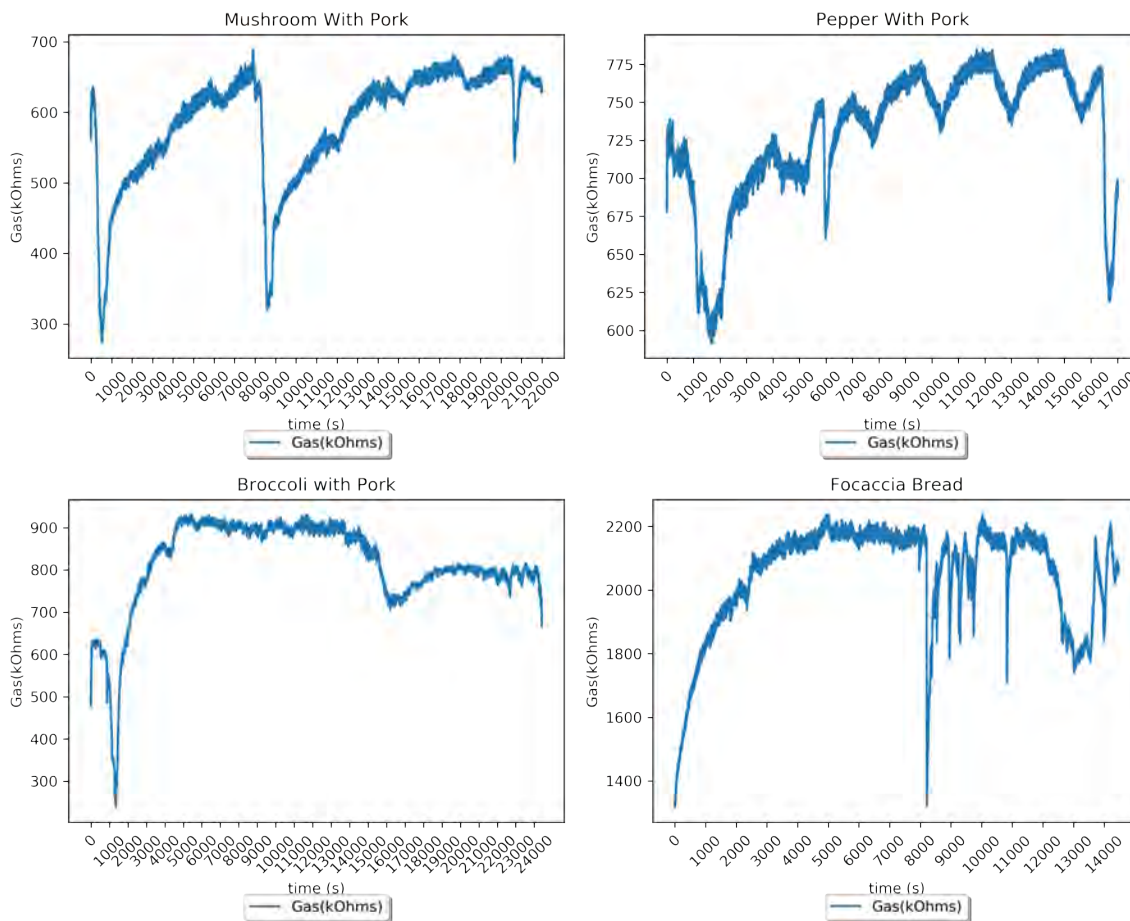


**Fig. 3.10.** Volatile Organic Compound Resistivity as measured by the BME680.

These plots show the VOC resistivity as measured from the BME 680. This value is inversely proportional to the PM concentration. One can see that it will spike down when PM concentration spikes up.

#### 4. Discussion

The results from our cooking trials behave in a mostly expected way, that is, when something is being cooked over heat, particulate matter (PM) concentrations are driven up. Across all runs we can see a similar pattern of PM concentration spikes followed by an exponential decay back to the baseline concentration. However, it is important to note that some events such as burning food might produce smoke. Smoke can drive PM concentrations significantly high and certain patterns in the data might be attributed to that.

We were able to extrapolate a few relationships between features in our data. Throughout all runs it can be seen that the VOC resistivity will spike at the same time as PM concentrations. Albeit, the VOC resistivity will spike down, i.e., its relationship with the PM concentration is inverse. We believe this is because the VOC sensor is also picking up the particulate matter but just

reading it in a different way. Another relationship we were able to pick out from collected data is a relationship between temperature and relative humidity. When temperature goes up, relative humidity will go down. Reference **Fig 3.9.** to view this relationship.

We were also able to extract some other interesting features from our data as well. While examining PM1.0, PM2.5, and PM10 readings, we were able to confirm that the readings all follow the same trend, that is, the fine details from each reading align. We were also able to do an analysis on the distribution of particle sizes. From this data we observed that in most cases, the distribution of particle sizes stayed the same. It would take the introduction of a new particle source to throw the distribution off. For example in the focaccia bread run, there is a change in particle distribution; this was due to non-stick cooking spray being used in the vicinity of the PM sensor. The effects of this distribution change are very short. We were also able to determine that cooking has no effect on the air pressure in the room, and air pressure had no effect on PM concentrations.

One thing that we were able to see in all of our runs involving cooking meat in an oil, was that each step in the cooking process could be seen as a spike in PM concentration (see **Fig 4.1.** and **Table 4.1**). We were able to reference our video logs to determine this. We saw that there was a spike in PM concentrations when oil was first introduced into the cooking vessel, as well as every time a new ingredient was added.

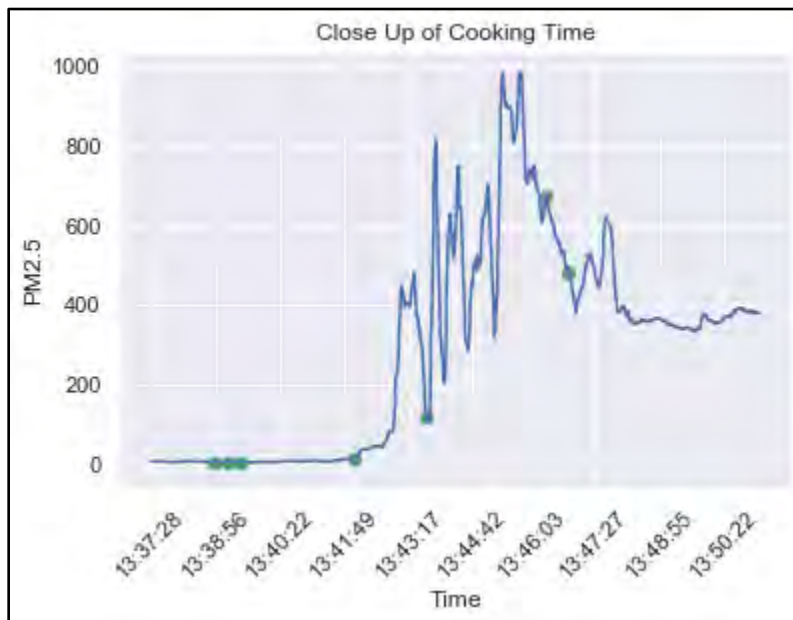


**Fig 4.1.** Zoomed in view of Mushroom with Pork PM spike.



**Table 4.1**

Timestamps and corresponding events.

Timestamp	Event
13:38:53	Mushroom added to boiling water
13:39:13	Pot removed from heat
13:39:30	Pot put back on heat
13:42:02	Oil added to pot
13:43:40	Mushroom added to pot
13:46:21	Sauce added to pot
13:46:51	Cooked pork added to pot

Our research shows that it is viable to build a data collection device and record the particulate concentration level in the home kitchen with an electric stove. We assumed the PM concentration would increase during the cooking process and would decay after the process. This assumption was indeed verified. We expect the increase of the concentration at the start of the cooking process and the decrease at the end to be exponential. The increase and decrease are indeed mostly exponential.

Previous studies have long established the harmful health effects of high concentration of particulate matter and that using fuel in cooking leads to a highly substantial increase in PM concentration. However, cooking using an electric stove is less understood. Our study, while neither comprehensive nor precise in nature, established that an appreciable increase in PM content would indeed arise during such a cooking process. It also established that it is possible to use easily acquired hardware and self-assembled circuits to collect data on such processes, enabling future and further studies to be conducted. However, we stress that until more controlled studies are conducted, it is impossible to draw conclusive and quantitative conclusions on how the PM concentration behaves during the cooking process.

We should also note here that during a specific cooking process, several factors might affect the behavior of PM concentration. As an example, if the kitchen is shared between several people, whether those people have used the kitchen before or after cooking might greatly impact how the PM concentration grows and decays, as can be seen in **Fig 4.2**. The baseline PM concentration before cooking can also have significant effects, as well as the use of ventilation. Environmental

factors like whether and how the kitchen is connected to other environments and random fluctuations in PM concentration, also need to be taken into account. We should also note that during certain kinds of cooking processes, open fire might be necessary, which would need to be studied and accounted for as well.

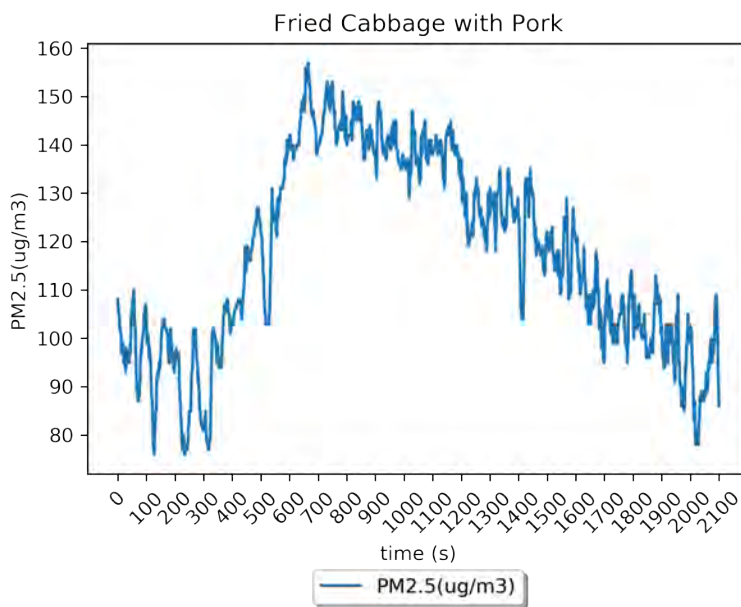


**Fig. 4.2.** Fried Cabbage with Pork PM2.5 concentration.

Given the limitations in our experimental resources and capabilities, we should note that during each data collection run, only one PMS5003 sensor and one BME680 sensor are used. While we strived to place them at a fixed distance from the stove, such things are not always possible in every setting. Using only one set of sensors also means we are unable to determine how changes in PM concentrations might differ between different distances from the stove. Moreover, while the BME680 sensor was used and in several experimental runs, the VOC gas resistance data returned from it can be seen to have the expected correlation with the PM concentration (see **Fig 3.2.** and **Fig 3.10.**), we do not have a clear and certain way to translate the data returned from the BME680 sensor, i.e., the resistance, into precise VOC concentration data. The resistivity might also be affected by factors such as humidity (Bosch 23), further clouding the use of VOC data to corroborate the PM data.

Furthermore, due to the circumstances during our experiments, it is impossible for us to gain access to a commercial kitchen and take data on cooking processes in such a kitchen, where the presence of possibly more people and the use of different ventilation systems might affect how the PM concentration grows and decays. However, if we assume these factors do not affect the behavior of PM concentrations too much, we may approximate the amount of PM a worker in the kitchen might be exposed to during an eight-hour shift. We present such data in the following table:

**Table 4.2**

Approximate average exposure of PM<sub>2.5</sub> and PM<sub>10</sub> in a commercial kitchen.

	PM <sub>2.5</sub> (Average, µg/m <sup>3</sup> )	PM <sub>10</sub> (Average, µg/m <sup>3</sup> )
Mushroom with Pork	217.57	263.61
Pepper with Pork	21.77	25.30
Focaccia Bread	3.07	3.74
Broccoli with Pork	66.79	77.83

In taking the average, we assumed each worker would perform the cooking process and then have a five-minute break before the next cooking process starts, i.e., the average considers the PM concentrations of the entire cooking process plus five minutes of baseline PM concentrations. In order to put the data into appropriate context, we compare the data with certain environmental standards. The Occupational Safety and Health Administration (OSHA) does not have a general indoor air quality standard (OSHA, “Indoor Air Quality in Commercial and Institutional Buildings” 11), and we were only able to compare our data with the general workplace air contaminants limits provided by federal regulations, which, at 15 mg/m<sup>3</sup> or 15,000 µg/m<sup>3</sup> (OSHA, “Limits for Air Contaminants”), far exceeds the spike value of any of our data runs. We also compared the data with the National Ambient Air Quality Standards (NAAQS) published by the EPA. Since the standards consider 24-hour average, we added a further 16-hour amount of baseline PM concentrations and re-calculated the average. The data and the NAAQS are as follows:

**Table 4.3**

Approximate 24-hour average exposure of PM<sub>2.5</sub> and PM<sub>10</sub> for a commercial kitchen worker and the NAAQS (EPA, “NAAQS Table”).

	PM <sub>2.5</sub> (24-Hour Average, µg/m <sup>3</sup> )	PM <sub>10</sub> (24-Hour Average, µg/m <sup>3</sup> )
Mushroom with Pork	75.86	91.87
Pepper with Pork	10.59	12.43
Focaccia Bread	1.69	1.91
Broccoli with Pork	24.93	28.61

NAAQS	35	150
-------	----	-----

According to the comparison, the “Mushroom with Pork” data run has a 24-hour average in PM<sub>2.5</sub> concentrations exceeding the NAAQS. Otherwise, all concentrations in our data are below the NAAQS. However, we urge readers to exercise caution in interpreting this result, as the NAAQS pertain to outdoor ambient air quality instead of indoor air quality.

Further research might be needed to concretely and accurately establish the behavior of PM concentration in a commercial kitchen. However, we believe it to be possible to develop a device for commercial kitchens that would alert when PM concentrations become unsafe. We also believe, given the lack of relevant governmental standards that we are aware of, it is important to further understand the issue and develop a reasonable regulatory or advisory standard to protect the health of commercial kitchen workers.

It is known that staying in an environment with a PM concentration higher than a certain level for an extended period of time could harm one’s health. However, we cannot verify how different levels of PM concentration might differ in how they negatively affect one’s health. We have no volunteers to stay in the kitchen for a long time so that we can observe how their health has been affected. This research could also be unethical if someone does get diseases by staying in the kitchen, and we possess no medical skills to diagnose their diseases. The process of causing a disease might also take years or decades. To study this situation, we believe further research could be conducted by surveying people who cook frequently. Though it might be still hard to rule out other possibilities that might lead to diseases.

We could not set up control groups either because it was impossible to set up perfectly identical situations. We could not control the wind flow or the internal shape of the kitchen which may affect the amount of the PM recorded by the sensor. We could not find the exact same steak or broccoli, and we could not make sure they are cooked in exactly the same way while keeping the environment unchanged. However, we think it is possible to replicate simple cases like cooking oil of the same volume inside a laboratory. In such a situation, it might be possible to study how different ingredients and cooking methods would affect PM concentrations differently.

Moreover, we do not have the capability to measure the temperature of the stove or the cooking container. Instead, we only know the power level of the stove. Even though we collected data on two cases with one using higher power and one using lower power and we found the one with higher power generated much higher concentrations of PM (Mushroom with Pork, see **Fig 3.2.**), we could only conclude that if other factors are negligible, the general trend is that higher power of the stove associates with higher PM concentrations. Further research might be needed to

establish exactly how temperatures of the cooking materials affect PM concentrations and find out if the correlation is positive or not, in ideal conditions.

## **5. Conclusion**

Based on our results, our study has achieved its aim, namely, to ascertain the feasibility of using easily acquired hardware and self-assembled circuits to measure PM concentrations during cooking processes in a kitchen setting. How cooking with an electric stove would affect PM concentrations is previously little understood, and we believe our results certainly demonstrate that further research in this area is possible.

Indeed, we have also observed several trends in PM concentrations. Among other things, we have seen that fine features in PM concentration data correspond to specific procedures in a cooking process, such as introducing a cooking ingredient. Moreover, we have seen the distribution of PM particle sizes varies little during the cooking processes, except in some cases where certain kinds of PM sources were introduced. We have also seen that in most cases PM concentrations decay exponentially after the cooking has concluded. Furthermore, we note that there might be a correlation between PM concentrations and VOC gas concentrations, which might warrant further research and might be used to further corroborate PM concentration data. We also note that air features such as air pressure, humidity, and temperature seem little affected by the cooking process. We caution that our results are by no means conclusive, and we view these results as illustrating general directions for further research.

We do believe, though, that our results can have practical implications. Since building such a data collection device is possible, commercial kitchens might be interested in developing such devices to alert their employees about possible unsafe PM concentrations. It might also be important to develop regulatory or advisory standards on PM concentrations in commercial kitchens. We again caution that we do not know for certain our results apply to commercial kitchens, given that all of our experiments were conducted in home kitchens and several factors possibly affecting PM concentrations might differ between commercial kitchens and home kitchens.

We also recommend further research looking into how PM concentrations might be affected by several factors, such as the use of ventilation, the temperature of the stove, and different cooking ingredients. Such research might need more controlled environments and possibly more specialized equipment that we do not have access to, but we believe our study has illustrated the general possibility of conducting these kinds of further research. It might also be important to further look into how the high PM concentrations caused by cooking affects human health, which is beyond the scope of our current study.

## **6. Acknowledgments**

The authors wish to thank George Gollin, Charlie Steiner, and Justin Languido for their instructions, support, and comments during the course of this study.

The authors wish to further thank George Gollin for his offer to let us collect data on ramen cooking in his kitchen, even though due to unforeseen circumstances we were unable to take this offer.

The authors also wish to thank Bevier Café for their offer to let us collect data in their facilities. The authors regret not being able to take this offer due to unforeseen circumstances.

### Works Cited

- Adafruit Industries. “3 x 4 Phone-style Matrix Keypad.” *Adafruit*, [www.adafruit.com/product/1824](http://www.adafruit.com/product/1824). Accessed 1 May 2020.
- . “Adafruit BME680 - Temperature, Humidity, Pressure and Gas Sensor.” *Adafruit*, [www.adafruit.com/product/3660](http://www.adafruit.com/product/3660). Accessed 30 April 2020.
- . “Adafruit DS3231 Precision RTC Breakout.” *Adafruit*, [learn.adafruit.com/adafruit-ds3231-precision-rtc-breakout/overview](http://learn.adafruit.com/adafruit-ds3231-precision-rtc-breakout/overview). Accessed 30 April 2020.
- . “INA219 High Side DC Current Sensor Breakout - 26V  $\pm$ 3.2A Max.” *Adafruit*, [www.adafruit.com/product/904](http://www.adafruit.com/product/904). Accessed 30 April 2020.
- . “MicroSD Card Breakout Board.” *Adafruit*, <https://www.adafruit.com/product/254>. Accessed 30 April 2020.
- . “PM2.5 Air Quality Sensor and Breadboard Adapter Kit - PMS5003.” *Adafruit*, [www.adafruit.com/product/3686](http://www.adafruit.com/product/3686). Accessed 30 April 2020.
- . “RGB Backlight Positive LCD 16 x 2 + Extras - Black on RGB.” *Adafruit*, [www.adafruit.com/product/398](http://www.adafruit.com/product/398). Accessed 30 April 2020.
- AirNow. *AirNow*, [www.airnow.gov](http://www.airnow.gov). Accessed 10 April 2020.
- Arduino. *Arduino*, [www.arduino.cc](http://www.arduino.cc). Accessed 30 April 2020.
- Bosch. “BME680 Low Power Gas, Pressure, Temperature & Humidity Sensor,” [cdn-shop.adafruit.com/product-files/3660/BME680.pdf](http://cdn-shop.adafruit.com/product-files/3660/BME680.pdf). Accessed 16 April 2020.

- Kim, Ki-Hyun, Kabir, Ehsanul, and Shamin Kabir. “A Review on the Human Health Impact of Airborne Particulate Matter.” *Environment International*, vol. 74, 2015, pp. 136-143.
- Kim, Hyungkeun, Kang, Kyungmo, and Taeyeon Kim. “Measurement of Particulate Matter (PM<sub>2.5</sub>) and Health Risk Assessment of Cooking-Generated Particles in the Kitchen and Living Rooms of Apartment Houses.” *Sustainability*, vol. 10, no. 3, 2018, pp. 843-855.
- Occupational Safety and Health Administration. “Indoor Air Quality in Commercial and Institutional Buildings.” *OSHA.gov*, [www.osha.gov/Publications/3430indoor-air-quality-sm.pdf](http://www.osha.gov/Publications/3430indoor-air-quality-sm.pdf). Accessed 28 April 2020.
- . “Limits for Air Contaminants.” 29 C.F.R. § 1910.1000 Table Z-1 (1989), [www.osha.gov/laws-regs/regulations/standardnumber/1910/1910.1000TABLEZ1](http://www.osha.gov/laws-regs/regulations/standardnumber/1910/1910.1000TABLEZ1). Accessed 28 April 2020.
- “PCB Layout.” *Learn EMC*, [learnemc.com/pcb-layout](http://learnemc.com/pcb-layout). Accessed 28 April 2020.
- Plantower Technology. “Digital Universal Particle Concentration Sensor – PMS5003 Series Data Manual,” [cdn-shop.adafruit.com/product-files/3686/plantower-pms5003-manual\\_v2-3.pdf](http://cdn-shop.adafruit.com/product-files/3686/plantower-pms5003-manual_v2-3.pdf). Accessed 30 April 2020.
- United States Environmental Protection Agency. “NAAQS Table.” *EPA.gov*, [www.epa.gov/criteria-air-pollutants/naaqs-table](http://www.epa.gov/criteria-air-pollutants/naaqs-table). Accessed 10 April 2020.
- . “Technical Assistance Document for the Reporting of Daily Air Quality – the Air Quality Index (AQI).” *EPA.gov*, [www3.epa.gov/airnow/aqi-technical-assistance-document-sept2018.pdf](http://www3.epa.gov/airnow/aqi-technical-assistance-document-sept2018.pdf). Accessed 2 April 2020.